

## THE STATUS OF Ka-BAND COMMUNICATIONS FOR FUTURE DEEP SPACE MISSIONS

C. Edwards, L. Deutsch, M. Gatti, J. Layland, J. Perret, C. Stelzried  
Jet Propulsion Laboratory, California Institute of Technology,  
M/S 303-402, 4800 Oak Grove Dr., Pasadena, California, 91109, USA  
Phone: 818-354-4408; Fax: 818-393-3573; E-mail: chad.edwards@jpl.nasa.gov

### Abstract

Over the past decade, the Jet Propulsion Laboratory's Telecommunications and Mission Operations Directorate has invested in a variety of technologies, targeted at both the flight and ground sides of the communications link, with the goal of developing a **Ka-band** (32 GHz) communications capability for future deep space missions. Driving this effort is the realization that moving from the current X-band (8.4 GHz) downlink frequency up to **Ka-band** offers roughly a four-fold performance improvement, providing a low-cost path for increasing the aggregate capacity of NASA's Deep Space Network and enabling new classes of small, low-cost microspacecraft. On the spacecraft, future radio systems, starting with the Small Deep Space Transponder, will offer the option of **Ka-band** exciters for downlink telemetry. Novel **Ka-band** antennas offer very high gain in low-mass, conformal packages, **Ka-band** Solid State Power Amplifiers have been demonstrated; however, significant improvements in both total output power and power-added efficiency are needed to achieve the full benefit of **Ka-band**'s performance advantages. On the ground, the DSN's new generation of 34-meter beam waveguide antennas has demonstrated both the aperture efficiency and precision pointing necessary to support **Ka-band** reception; current efforts are focused on assessing the potential utility of the 70m antennas at 32 GHz. Multi-year radiometry at all three DSN sites provides a statistical assessment of **Ka-band** atmospheric effects. And a series of flight demonstrations, including the current **Ka-band** Link Experiment on the Mars Global Surveyor spacecraft, have validated our end-to-end understanding of the communications link.

### 1. Introduction

The Jet Propulsion Laboratory (JPL), operated by the California Institute of Technology for the National Aeronautics and Space Administration (NASA), is NASA's lead center for the robotic exploration of the solar system. The Telecommunications and Mission Operations Directorate at JPL is responsible for end-to-end communications, and in this role invests in space and ground communications technologies to improve the performance and reduce the cost of deep space communications.

Because of the extremely large distances involved in planetary exploration, communications represents one of the most challenging aspects of deep space missions. To put this in perspective, a spacecraft at Pluto is more than 100,000 times farther from Earth than a typical geostationary communications satellite. Because signal strength decreases as the square of distance, simply moving that geostationary satellite to Pluto with no changes in the spacecraft or ground communications systems would result in a reduction in link performance by more than a factor of 10 billion. To compensate for this, deep space communications links are characterized by highly directional spacecraft antennas and by the very large aperture ground antennas and extremely sensitive receiving systems of the Deep Space Network (DSN).

The future deep space mission set reflects a move towards much more frequent, lower-cost missions. These missions are characterized by ambitious science goals requiring large data volumes on the space-to-ground link. At the same time, these missions must be accomplished at much lower cost than previous deep space missions, driving the design of smaller, cheaper spacecraft in which the mass and power of each subsystem must be minimized. And the growing mission set must be supported by an already oversubscribed ground network. Finally, NASA is moving to a philosophy of full cost accounting for each flight project, in which the project budget must reflect all of the costs associated with the mission, including the cost of ground tracking resources. This will drive future flight projects to explore flight-ground trades to allow minimizing the hours of DSN tracking time they require.

In response to these considerations, TMOB is investing in flight and ground technologies to make Ka-band (32 GHz) space-to-ground communications viable for future deep space missions. Relative to the current X-band (8.4) downlink channel, Ka-band offers significantly improved link performance, primarily due to the narrower beamwidth (for a given spacecraft antenna size) of the downlink signal, focusing more power on the Earth receive station. Future missions can take advantage of this increased link performance by increasing the downlink data rate, reducing required tracking time, using smaller, cheaper ground tracking antennas, and/or reducing the mass, volume, and power of the spacecraft communications system [Hemmati et al., 1997].

The data rate  $R$  supportable on an RF link between two directional antennas scales as

$$R \propto P_T \epsilon_T \left( \frac{D_T}{\lambda} \right)^2 \left( \frac{D_R}{L} \right)^2 \frac{\epsilon_R}{T_R}$$

where

$P_T$  = the transmitted power;

$\epsilon_T$  = the transmission efficiency (including power amplifier, antenna, and other system losses);

$D_T$  = the diameter of the transmitting antenna;

$\lambda$  = the RF transmission wavelength;

$D_R$  = the diameter of the receiving antenna;

$L$  = the distance between the transmitter and receiver;

$\epsilon_R$  = the aperture efficiency of the receiving antenna; and

$T_R$  = the system noise temperature of the receiver.

This link equation illustrates the performance advantage of higher frequencies and shorter wavelengths. In a sense, the communications wavelength sets a scale for the size of the spacecraft communications system, as the directivity of the spacecraft antenna is determined by its diameter, measured in units of wavelength. In other words, a 50-cm antenna operating at Ka-band (32 GHz) will have the same beamwidth as a 2-meter antenna operating at X-band (8 GHz). Thus for a given directivity, the linear dimensions of the antenna scale with wavelength  $\lambda$ , with mass and volume scaling roughly as  $\lambda^3$ . Other microwave components (waveguide, duplexers) will also be reduced in mass and volume at higher frequencies. Alternatively, the higher directivity of the Ka-band beam, for a fixed antenna size, can be used to increase the data rate for a given spacecraft mass and volume. Mission designers can take advantage of this inherent link advantage by increasing data rate and/or by reducing spacecraft power, mass, and volume. These considerations have driven future mission interest in Ka-band as a deep space communications frequency, particularly for the space-to-ground link.

Ka-band offers additional advantages in terms of the reduced effects of charged particles in the solar plasma and the Earth's ionosphere. This allows Ka-band to offer the potential for improved communications performance at low Sun-Earth-probe angles for missions such as NASA's Solar Probe [Feria, et al., 1997], and will enable greatly improved radio science accuracy for occultation studies and gravitational wave searches in the upcoming Cassini mission [Comoretto, et al., 1992].

Based on the above equation, one would naively expect communications link performance to scale inversely as  $\lambda^2$ , implying a 12 dB advantage for Ka-band relative to X-band. However, decreases in spacecraft transmitter efficiency, increased spacecraft pointing losses due to the narrower downlink beam, increased atmospheric attenuation and noise temperature, decreased ground aperture efficiency, and increased ground antenna pointing losses and receiver noise reduce the overall link advantage. After accounting for these losses, Ka-band still offers performance improvements of up to 6 dB. The goals of the TMOB technology program have been to develop flight and ground technologies to maximize this Ka-band link advantage and to quantify end-to-end Ka-band link performance in actual flight demonstrations.

## 2. Spacecraft Systems

A central element of the spacecraft telecommunications system is the transponder, which amplifies, receives, and demodulates the **uplink** radio signal, and coherently generates a **downlink** signal which is modulated with the spacecraft telemetry. Other essential components of the spacecraft radio systems are the spacecraft antenna(s), the **diplexer** which separates the **uplink** and downlink signals, and the power amplifier for the downlink signal. Whereas antennas, **diplexers**, and power amplifiers vary significantly from mission to mission, due to mission data rate requirements, range from Earth, and spacecraft configuration issues, a single transponder design can meet the needs of most deep space missions. In addition, the transponder has historically been the most expensive element in the spacecraft telecommunication system. Previous deep space transponders have supported 2.3 and 8.4 GHz links; two new transponder developments will, for the first time, provide standard Ka-band downlink options for future missions.

The Small Deep Space Transponder (SDST), being developed at JPL under a contract to Motorola, will provide a near-term solution for missions beginning with the 1998 New Millennium DS I mission. Integrating the Command Detector Unit (CDU) and Telemetry Modulation Unit (TMU) functions into the transponder architecture for the first time, the SDST will achieve more than a factor of two reduction in mass and nearly a 70% reduction in volume relative to the Cassini Deep Space Transponder, CDU, and TMU. In addition, the SDST is projected to achieve a factor of two or more reduction in recurring unit cost, due largely to reduced parts count resulting from the use of digital and RF integrated circuits. The SDST supports an X-band **uplink** and X- and Ka-band downlinks. Key technologies reflected in the SDST design include advanced multi-function GaAs MMIC devices, Multi-Chip Modules incorporating Low-Temperature Co-Fired Ceramic substrates, and a fully digital ASIC baseband receiver. The engineering model of the SDST was delivered to the New Millennium DS I project in July, 1997.

In parallel with the SDST development, the conceptual design and breadboard development of an even more ambitious next-generation transponder, which will also support Ka-band downlinks, is taking place. This transponder, referred to as the Spacecraft Transponding Modem (STM), aims for order-of-magnitude reductions in mass and volume relative to the Cassini-era radio system, while also achieving significant further reductions in power relative to the SDST. The STM relies on an innovative architecture approach which minimizes the complexity of the RF sections and moves the majority of the transponder functionality into digital circuitry. The RF circuitry is reduced to a small number of MMIC chips, housed in Multi-Chip Modules, and the digital circuits will consist of two custom ASICs. It is anticipated that the number of parts in the STM will be a factor two to five lower than SDST, resulting in considerable further reduction in recurring cost. Other unique features of the STM include a frame-level interface between the transponder and the flight computer, regenerative ranging capability, integrated channel (error-correcting) coding, and provision of time and frequency references for use by other spacecraft systems. A demonstration of a breadboard of the STM is planned for 1997, and further development will be targeted toward a flyable prototype by the year 2000.

Solid State Power Amplifiers (SSPAs) are currently the device of choice for generating the downlink RF signal strength, due to their high reliability as well as their low size and cost. X-band devices are currently providing efficiencies of 25%. In order to fully realize the benefits of Ka-band, the efficiency of Ka-band SSPAs will have to be improved, using the latest device technology, such as pseudomorphic high electron mobility transistors (PHEMTs). JPL has developed a flyable 1.5 W Ka-band SSPA breadboard, shown in Figure 1, with 32 dB gain and a power-added efficiency of 16% (not including the DC-DC power converter losses) [Wamhof, et al., 1994]. Lockheed Martin has demonstrated a 1.5 W device with a power added efficiency of 20% as a breadboard demonstration for the Pluto Express mission. Because individual SSPA devices are limited in output power, achieving high power and high efficiency has been difficult due to microstrip losses in combining the outputs of several parallel devices. Higher output power levels and increased efficiencies are being pursued through the use of quasi-optical combining systems to allow free-space combining of transmitted power from an array of solid-state amplifiers. This may provide a path for 10W, 40% efficient SSPA-based Ka-band transmitters. An alternative approach to higher transmitter power and efficiency is to revisit the traveling wave tube (TWT) design that is being flown on Cassini, taking advantage of recent packaging improvements to greatly reduce the mass, volume, and cost of the Ka-band TWT. This could provide a low-risk path to a 10W, 40% efficient transmitter in the 2000 time frame.

A dual-frequency X/Ka-band feed has been developed by Lockheed Martin Astronautics to illuminate the parabolic Cassegrain antenna on the Mars Global Surveyor spacecraft. In addition to this straightforward approach to Ka-band antennas, JPL has also investigated reflectarray antennas as an approach to achieving low mass that is particularly well-suited to integrating the high-gain antenna into the spacecraft bus structure. The reflectarray uses a flat array of passive patch elements to emulate a parabolic reflector. The result is a flat, very low-mass antenna that can be built right onto a flat surface of a microspacecraft bus structure. By illuminating the patch elements with a microwave feed, the reflectarray avoids the large distribution losses that plague microstrip patch antennas at higher frequencies. A O. S-meter 32-GHz breadboard reflectarray antenna, shown in Figure 2, was completed in 1996 [Huang and Pogorzelski, 1997], and current work is focused on integrating the reflectarray concept into an inflatable membrane structure for large-aperture, low-mass, and low-stowed-volume applications.

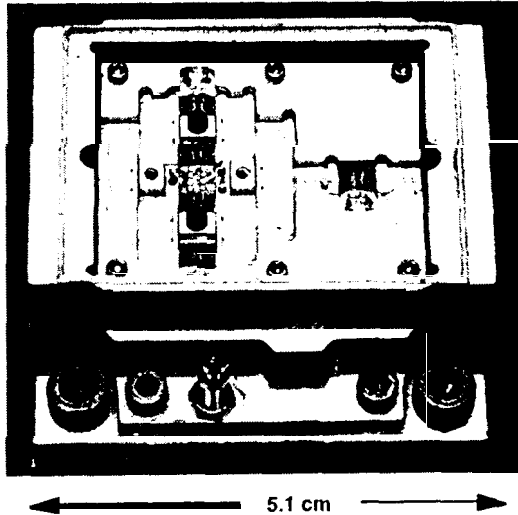


Figure 1: 1.5-Watt 32-GHz Solid State Power Amplifier

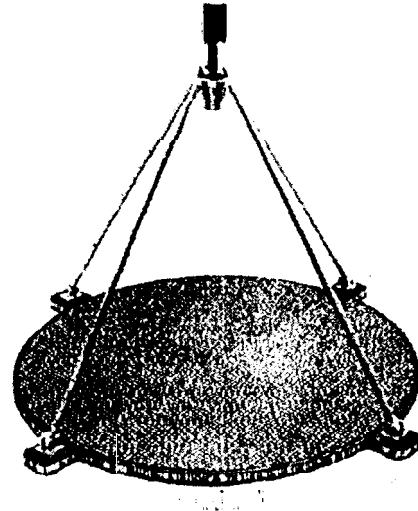


Figure 2: O. S-meter 32-GHz Reflectarray Antenna

### 3. Ground Systems

In concert with subsystem developments on the spacecraft, key developments on the ground side of the telecommunications link are underway to meet the needs of future deep space missions. The DSN's R&D antenna facility, DSS 13 at Goldstone, CA, is the prototype for a new family of 34-m Beam WaveGuide (BWG) antennas in the DSN which will support 32GHz space-to-ground links. The BWG design focuses the collected RF signal onto a small hole in the primary reflector surface, after which a series of RF mirrors direct the energy to a room in the pedestal of the antenna. As shown in Figure 3, the BWG approach allows the RF receiving systems to be located in a stable, easily accessible laboratory environment.

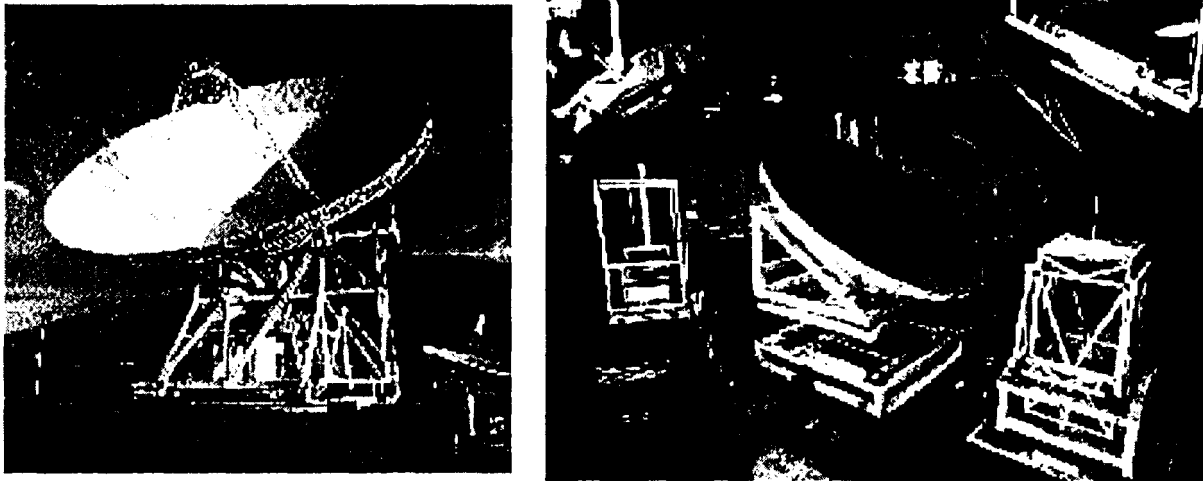


Figure 3: DSS 13, the DSN'S 34m R&D Beam Waveguide Antenna, and the pedestal area beneath the antenna where multiple microwave feed packages can be illuminated by the central rotating mirror.

DSS 13 has provided a testbed for developing and demonstrating Ka-band ground systems and for quantifying the advantages of Ka-band relative to X-band. With roughly a four-times smaller wavelength, Ka-band operations provide significant challenges in antenna pointing and in antenna surface accuracy. An antenna pointing error of 5 millidegree or an RMS surface error of 0.38 mm will lead to a Ka-band loss of 1.0 dB at Ka-band. These challenges are being met by a variety of new developments.

First, the new generation of 34m BWG Antennas are specifically being designed with Ka-band performance in mind. The structures are very stiff, to avoid gravity-induced surface deformations, and the individual antenna panels are built to much tighter tolerances. RF holography is being used to accurately adjust the panel settings, achieving RMS surface accuracies of 0.3 mm at the antenna rigging angle [Rochblatt, et al., 1995]. To correct for any residual gravity-induced surface distortions, several approaches are being investigated, including mechanical compensation forces applied to the antenna backup structure [Strain, et al., 1997] and deformable mirrors in the beam waveguide optics. Pointing needs are being met with a combination of improved blind pointing algorithms, development of a monopulse Ka-band tracking feed [Lo, 1996], and use of conical scanning about the boresight, using one of the mirrors in the beam waveguide optics as a fine-steering mirror. A final development, which provides both closed-loop pointing and surface compensation, is the array feed [Vilnrotter and Iijima, 1996]. This array of seven Ka-band feeds (one central feed surrounded by a ring of six feeds) collects a defocused or mispointed Ka-band beam. By correlating the signals between each pair of feeds, the relative phase and amplitude of the signal in each of the seven feeds is determined. Based on these measurements, the defocused signal can be optimally re-combined, and the pointing information fed back to the antenna pointing system to keep the signal focused on the central feed. Each of these approaches is currently being developed and demonstrated on the 34m DSN R&D antenna; in the coming years, several of these approaches will also be tested on the 70m antenna to determine the potential Ka-band performance of these larger apertures.

Ka-band is more susceptible to atmospheric effects, including absorption and increased atmospheric noise temperature, than X-band. Water Vapor Radiometers are deployed at each of the DSN sites to collect information on brightness temperature statistics. Several years of data are now available from each complex and are being used to develop a Ka-band weather model which can be used to design reliable Ka-band deep space communications links [Harcke, et al., 1996].

All of these developments come together in an ongoing program of Ka-band observations using the DSS-13 R&D station. To date, over 1000 simultaneous X/Ka-band observations of natural radio sources (planets and quasars) have been made with the goals of quantifying the overall link advantage for Ka-band relative to X-band, characterizing antenna and atmospheric losses at Ka-band, and quantifying incremental improvements in Ka-band BWG performance [Morabito, 1996]. Figure 4 presents the results of these observations, which are characterized by a peak 57% Ka-

band aperture efficiency at 40 deg elevation, and an overall 6-8 dB Ka-band link advantage for the ground system, including atmospheric effects. The plots depict the measured ratio of antenna gain to system noise temperature (G/T), the figure of merit for a communications system, for both X-band and Ka-band. The plotted values have been corrected to reflect planned X- and Ka-band low noise amplifier improvements. The curvature of the measured G/T response exhibits the characteristic roll-off due to gravity effects away from the 45 deg rigging angle of the antenna where the panel setting is optimized, and also reflects the increased noise temperature due to atmospheric effects at low elevations. The spread of the data in the vertical (G/T) direction is a measure of the variability of the system performance, due largely to weather variations; the greater impact of weather on the Ka-band link is evident.

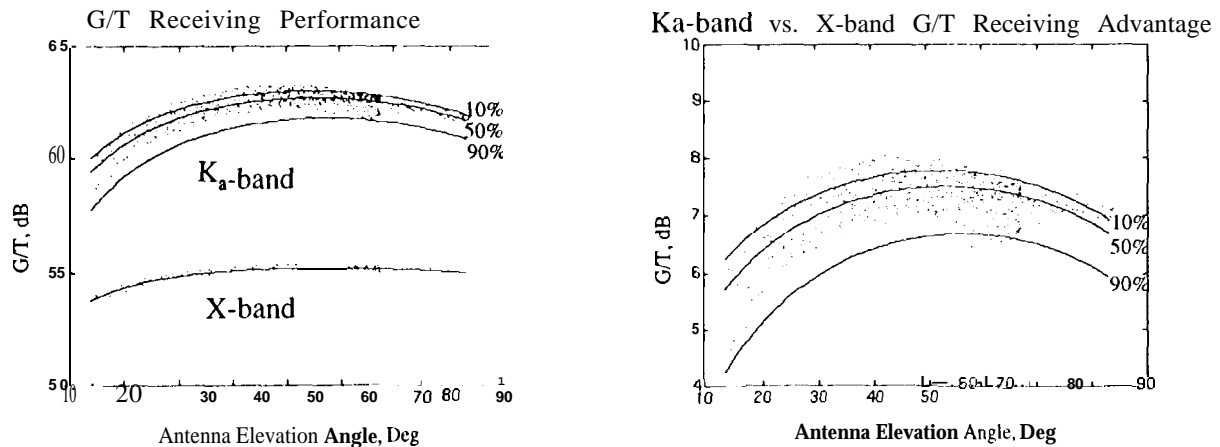


Figure 4: Ratio of antenna gain to system noise temperature (G/T) measured at X- and Ka-band on the DSS- 13 DSN 34-m B WG antenna at Goldstone, CA. Data represent over 1000 boresight observations of natural radio sources. The plot on the right displays the difference of the Ka- and X-band curves, representing the advantage of the Ka-band ground system with respect to X-band. The data have been scaled to reflect projected low noise amplifier noise temperatures of 13 K for Ka-band and 6 K for X-band. The solid curves indicate theoretical predictions, with percentile labels for different assumptions for the cumulative weather distribution.

#### 4. Flight Demonstrations

To demonstrate the readiness of Ka-band flight and ground systems, TMOD is carrying out a series of Ka-band flight demonstrations. The Mars Observer spacecraft carried the Ka-Band Link Experiment (KaBLE)[Rebold, et al., 1994], a flight experiment sponsored by TMOD which demonstrated the first deep space Ka-band downlink, prior to the loss of the spacecraft just prior to Mars encounter. With an EIRP of only 47 dBm, this experimental downlink provided sufficient power for carrier acquisition, but could only support low-rate telemetry and ranging early in the Earth-Mars cruise. Nevertheless, this demonstration was very successful in providing a first look at end-to-end Ka-band performance.

The Student Undergraduate Research Fellowship Satellite (SURFSAT) is a student-built flight experiment, sponsored by TMOD and launched on November 4, 1995 as a secondary payload aboard the Delta-11 second stage of the RADARSAT launch vehicle. Orbiting the Earth at an altitude of 1000-1400 km, SURFSAT radiates X-band, Ku-band, and Ka-band beacons for use in assessing the performance of DSN ground systems. SURFSAT has been very useful in providing a target for testing Ka-band ground system performance, and has also been critical in testing the X- and Ku-band links on the DSN's new Space VLB1 antennas.

Most recently, TMOD has sponsored a second Ka-Band Link Experiment (KaBLE-II) aboard the Mars Global Surveyor (MGS) spacecraft [Butman, et al., 1997]. With the addition of a 1-Watt SSPA and a dual-frequency X/Ka-band feed illuminating the full MGS high-gain antenna, KaBLE-II achieves an EIRP of 76 dBm, much larger than the original KaBLE experiment. The resulting Ka-band downlink supports Doppler, ranging, and high-rate telemetry at Mars distances. Already during cruise, MGS/KaBLE-II has validated the expected end-to-end link performance and

provided successful demonstrations of Ka-band Doppler and ranging data. The KaBLE-II experiment will continue throughout the MGS mapping phase, including data collection at solar conjunction to assess the improved performance of Ka-band telemetry at low Sun-Earth-probe angles. And in the near future, the New Millennium Deep Space 1 mission will continue this progression of Ka-band flight demonstrations with an experimental Ka-band downlink, utilizing the new Small Deep Space Transponder.

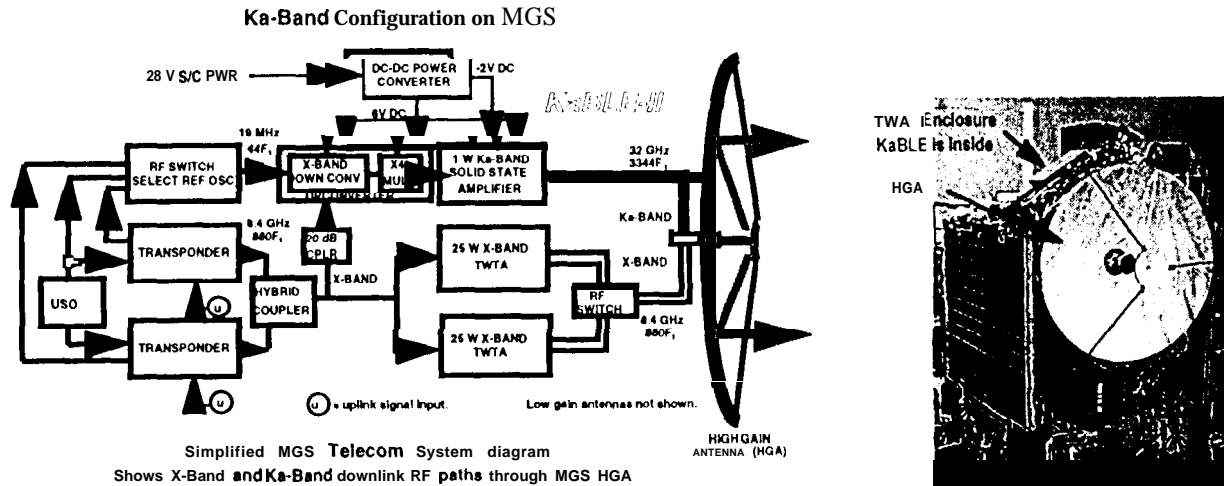


Figure 5: Block diagram of the MGS/KaBLE-II flight system and final flight hardware integrated on MGS.

## 5. Future Plans

After Mars Orbit Insertion in September, 1997, the Mars Global Surveyor KaBLE-II experiment will continue to collect Ka-band data at the DSS 13 research and development station during the mapping phase of the mission. In 1998, the first fully operational Ka-band system will be installed at DSS 25, one of the new operational beam waveguide antennas at Goldstone, based on the DSS 13 prototype. MGS/KaBLE-II will serve as a valuable test satellite for verifying the operational readiness of the DSS 25 Ka-band system. The first operational Ka-band support at DSS 25 will be for the Ka-band downlink on the New Millennium DS1 spacecraft, with a planned launch date of July 1, 1998.

Subsequently, the feed systems at DSS 25 will be upgraded to add a Ka-band uplink capability and allow simultaneous transmission and reception at both X- and Ka-bands, in order to support the Cassini Radio Science experiment. The X/X/Ka/Ka operation will be utilized during the Cassini cruise phase to search for gravitational radiation, starting in 2000. Installation of Ka-band systems at DSS 34 in Canberra and DSS 54 in Madrid is currently in TMOD'S implementation plans, providing round-the-globe Ka-band deep space reception by 2002.

Technology developments at DSS 13, and flight demonstrations with Mars Observer, SURFSAT, and Mars Global Surveyor, have established the readiness of the Deep Space Network to support Ka-band space-to-ground links. Ka-band offers future mission designers new options in increasing data return or reducing the size of future spacecraft communications systems. Targeted technology investments in the coming years to improve the efficiency of Ka-band spacecraft transmitters will play a key role in further maximizing the overall link advantage of Ka-band relative to current X-band systems. Based on this advantage, future missions should seriously consider Ka-band space-to-ground links in terms of their potential for performance enhancement or cost reduction relative to conventional X-band deep space links.

## Acknowledgements

The work described in this paper was performed at the Jet Propulsion Laboratory, California Institute of Technology under contract with the National Aeronautics and Space Administration.

## References:

Butman, S., D. Morabito, A. Mittskus, J. Border, J. Berner, C. Whetsel, M. Gatti, C. Foster, V. Vilnrotter, H. Cooper, A. Del Castillo, A. Kwok, J. Weese, M. Speranza, R. Davis, W. Adams, A. McMechen, C. Goodson, G. Bury, D. Recce, "Mars Global Surveyor Ka-band Link Experiment," Third Ka-Band Utilization Conference, Sorrento, Italy, September 15-18, 1997.

Comoretto, G., B. Bertotti, L. Iess, and R. Ambrosini, "Doppler Experiments with Cassini Radio System," *Il Nuovo Cimento*, Vol 15 C, N. 6, pp. 1193-1198, 1992.

Feria, Y., M. Belongie, T. McPheeters, and H. Tan, "Solar Scintillation Effects on Telecommunication Links at Ka-Band and X-Band," The Telecommunications and Data Acquisition Progress Report 42-129, May 15, 1997.

Harcke, L. J., P. F. Yi, M. K. Sue, and H. H. Tan, "Recent Ka-Band Weather Statistics for Goldstone and Madrid," The Telecommunications and Data Acquisition Progress Report 42-125, May 15, 1996.

Hemmati, H., K. Wilson, M. K. Sue, L. J. Harcke, M. Wilhelm, C.-C. Chen, J. R. Lesh, Y. Feria, D. Rascoc, F. Lansing, and J. W. Layland, "Comparative Study of Optical and Radio-Frequency Communication Systems for a Deep-Space Mission," The Telecommunications and Data Acquisition Progress Report 42-128, Feb 15, 1997.

Huang, J. and R. Pogorzelski, "Microstrip Reflectarray With Elements Having Variable Rotation Angles," Digest of the IEEE Antenna and Propagation Society International Symposium, Montreal, Canada, pp. 1280-1283, July, 1997.

Lo, V. Y., "Ka-Band Monopulse Antenna-Pointing Systems Analysis and Simulation," The Telecommunications and Data Acquisition Progress Report 42-124, February 15, 1996.

Morabito, D. D., "The Efficiency Characterization of the DSS-13 34-Meter Beam-Waveguide Antenna at Ka-Band (32.0 and 33.7 GHz) and X-Band (8.4 GHz)," The Telecommunications and Data Acquisition Progress Report 42-125, May 15, 1996.

Rebold, T. A., A. Kwok, G. E. Wood, and S. Butman, "The Mars Observer Ka-Band Link Experiment," The Telecommunications and Data Acquisition Progress Report, pp. 250, May 15, 1994.

Rochblatt, D. J., P. M. Withington, and H. J. Jackson, "DSS-24 Microwave Holography Measurements," D. J. Rochblatt, P. M. Withington, and H. J. Jackson, The Telecommunications and Data Acquisition Progress Report 42-121, May 15, 1995

Strain, D. M., L. S. Alvarez, M. Moore, and S. Stewart, "Cammatic: Automated Compensation for DSS-13 Antenna Gravity-Loading Performance Degradation," The Telecommunications and Data Acquisition Progress Report 42-129, May 15, 1997.

Vilnrotter, V. and B. Iijima, "Analysis of Array Feed Combining Performance Using Recorded Data," The Telecommunications and Data Acquisition Progress Report 42-125, May 15, 1996.

Wamhof, P. D., D. L. Rascoe, K. A. Lee, and F. S. Lansing, "A 32-GHz Solid-State Power Amplifier for Deep Space Communications," The Telecommunications and Data Acquisition Progress Report 42-117, pp. 236-249, May 15, 1994.